Swelling Kinetics of Linseed Oil-Based Nanocomposites

Vinay Sharma,[1,2] J. S. Banait,[2] P. P. Kundu[1]

[1]Department of Chemical Technology, Sant Longowal Institute of Engineering & Technology, Sangrur 148106, Punjab, India
[2]Faculty of Physical Sciences, Punjabi University, Patiala 147002, Punjab, India

ABSTRACT: The solvent-resistance properties of the montmorillonite-filled conjugated linseed oil-based nanocomposites are studied in tetrahydrofuran through equilibrium swelling method at different temperatures. The values of "n" in solvent transport equation are found to be below "0.5," showing the non-Fickian diffusion in the polymer. The dependence of the diffusion coefficient on the composition, percentage of clay, and temperature has been studied for nanocomposite samples. The diffusion coefficient increases with an increase in the clay contents and temperature. The crosslink density of the nanocomposites ranges from 101.07 to 237.46 $\times$ 10^6 mol/cm^3. © 2009 Wiley Periodicals, Inc. J Appl Polym Sci 114: 446–456, 2009

Key words: conjugated linseed oil; nanocomposite; montmorillonite; sorption; non-Fickian diffusion

INTRODUCTION

Polymer nanocomposites are the future of the global industries.[1] The polymer nanocomposites are prepared by dispersing a nanofiller into the polymer.[2,3] These platelets are then distributed into a polymer matrix creating multiple parallel layers. These platelets force flow of gases and liquids through the polymer in a torturous path, forming a complex barrier.[4] Different types of fillers are used for the preparation of nanocomposites. Among these, the most common is a nanoclay called montmorillonite—a layered smectite clay.[5–10] Additional nanofillers include carbon nanotubes, graphite platelets, carbon nanofibers, etc.[8,11–13] The barrier properties of the nanocomposites are supposed to increase due to nanoclay loading.[4,14]

The swelling technique is an easy and commonly used method to determine various coefficients such as diffusion, sorption, and permeability coefficient.[15–19] In swelling experiments, the polymer of known dimension is dispersed in a solvent, the solvent mass uptake versus time is recorded, and the data are used to calculate the various coefficients. These coefficients give an idea about the use of polymers in various applications, such as membranes, ion exchangers, controlled release systems, packaging, microchip manufacture, etc.

Sorption kinetics in polymers exhibit a variety of deviations from normal Fickian behavior, attributable to (a) slow viscous relaxations of the swelling polymer or (b) differential swelling stresses generated by the constraints imposed on local swelling during sorption. Several models have been proposed for the study of swelling behavior of the polymers.[20–22] *In situ* study by FTIR-ATR is also performed by many researchers for the prediction the sorption behavior of the polymers.[23–25]

In this study, a new system of linseed oil-based nanocomposites is studied using Fickian model. The variation in sorption is studied with respect to temperature. The rationale of this work is to study the sorption and diffusion kinetics of the nanocomposites based on linseed oil with an alteration in the oil and clay contents. The mechanism of the sorption is studied from the data by the linear fit of the equation of the transport phenomena. The effect of nanofiller on the barrier properties of the composites is also studied. The crosslink density and molecular weight between two crosslinks are also calculated from the sorption data using Flory-Rehner equation.

EXPERIMENTAL

Materials

Conjugated linseed oil (87% conjugation) is purchased from Alnor Oil Company, NY. Acrylic acid and tetrahydrofuran are purchased from Merck Chemical Co., Germany. Divinylbenzene is purchased from Fluka Chemie. Montmorillonite (K-10), cetyl trimethyl ammonium bromide, hexadecyl ammonium bromide are purchased from Aldrich

TABLE I
Detailed Composition of the Polymer Samples Prepared from Linseed Oil

Sample ID	Conjugated linseed oil (%)	Divinylbenzene (%)	Acrylic acid (%)	Clay montmorillonite[a] (K-10) (%)
CLin30	30	10	60	5(CTAB)
CLin40	40	10	50	5(CTAB)
CLin50	50	10	40	5(CTAB)
CLin60	60	10	30	5(CTAB)
CLin70	70	10	20	5(CTAB)
CTABMONT2.5	50	10	40	2.5(CTAB)
CTABMONT7.5	50	10	40	7.5(CTAB)
CTABMONT10	50	10	40	10(CTAB)
HDABMONT2.5	50	10	40	2.5 (HDAB)
MONT0	50	10	40	0

[a] The clay is modified by using cetyl trimethyl ammonium bromide (CTAB), or hexadecyl ammonium bromide (HDAB).

Chemical Company (Milwaukee, MI) and are used as received.

Sample preparation

Modification of montmorillonite

Montmorillonite clays are dispersed in DI water by stirring. Cetyl trimethyl ammonium bromide (CTAB) or hexadecyl ammonium bromide (HDAB) is added to dispersion. The whole dispersion is heated at 80°C for 4 h. The exchanged clays are filtered and washed with DI water, until it is free from bromide (tested and titrated by silver nitrate). The modified clay is dried at 80°C under vacuum. Cation-exchange capacity calculated from the titre value for CTAB is 29.92 and for HDAB 152.84 meq/100 g of clay.

Nanocomposite preparation

The polymeric nanocomposites have been prepared by heating the desired mixture of conjugated linseed oil, acrylic acid, and divinylbenzene and modified montmorillonite in a glass vial. The modified nanofillers of a predetermined quantity are dispersed in conjugated linseed oil–acrylic acid–divinylbenzene. The detailed compositions are reported in Table I. The dispersion is maintained by constant magnetic stirring at 500 rpm (overnight for proper intercalation). The mixture is heated at 85°C for 2 h, followed by at 95°C for 1–4 h such that the viscosity of the liquid (prepolymer) is sufficiently high and fillers got totally exfoliated. At this condition, the fillers will not be separated from the prepolymer even on stopping stirring. The whole mass is transferred to an appropriate mold and put in a heated oven at 100°C for 2 h and 120°C for 12 h and 130°C for 12 h.

Swelling experiments

The samples are cut into circular form, using a die of 12 mm diameter. The thickness of the samples is measured by means of a screw gauge. The dry samples are weighed on an electronic balance and then kept in the solvent in screwed bottles. The samples are taken out of the solvent at specific intervals and the excess solvent is rubbed off. The samples are then weighed and again immersed in the solvent, till equilibrium is attained (i.e., 72 h). The time for measuring weight of the sample is kept minimal (about 30 s), so that the escape of solvent from the sample is negligible. Equilibrium swelling experiments at different temperature are carried out at 25, 30, 35, and 40°C (±1°C) to study the effect of temperature on swelling. For temperatures higher than room temperature, the samples are kept in a microprocessor controlled hot air oven.

The mole percent uptake (Q_t) at each time interval is calculated by using eq. (1).[26]

$$Q_t = \frac{M_t}{M_r} \times \frac{100}{M_i} \qquad (1)$$

where M_t is the mass of solvent taken up at time t, M_r is the relative molar mass of the solvent and M_i is the mass of the dry sample.

Equilibrium swelling experiments are also performed at 25 ± 1°C to determine the solubility parameter of samples prepared by cationic and thermal polymerization. The swelling is carried out in various solvents ranging from 8.91 to 14.51 (cal/cm^3)$^{1/2}$. From the plots of equilibrium swelling volume (Q_t) versus solubility parameter (δ), tetrahydrofuran gives the maximum value of Q in all the samples and, hence, is used for further kinetic studies. Figure 1 shows the representative plot of volume equilibrium swelling versus solubility parameter for CLin 50 sample.
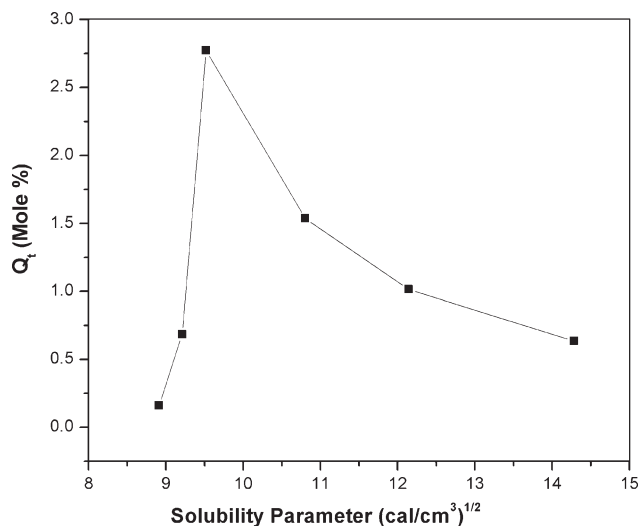
Figure 1 Plot of volume equilibrium of swelling (Q) versus solubility parameter (δ) for Lin50 and CLin50 samples at 25°C. The δ values in $(cal/cm^3)^{1/2}$ of the used solvents are 8.91 (toluene), 9.21 (chloroform), 9.52 (THF), 10.8 (dimethyl acetamide), 12.14 (dimethyl formamide), and 14.28 (methanol).

Optical characterization of swelled samples

The samples are monitored through an optical microscope (Digital Blue-QX5, PC Controlled). The swelled samples are observed through optical microscope and photographs are taken at 100 μm scale at different magnifications (60 and 200 X).

RESULTS AND DISCUSSION

Swelling of polymer samples

Effect of temperature

The mole percent uptake of the solvent is plotted against square root of time. The samples are studied for the change in sorption due to the change in temperature (25, 30, 35, and 40°C) and are shown in Figures 2–9. It is observed that the solvent uptake decreases with an increase in temperature. Figures 2 and 4 show a noticeable decrease in solvent uptake up to 50% increase in the oil contents, followed by a little decrease. On moving from Figures 2–8, nearly 50% decrease in the solvent uptake is observed. It is known that the layered nanofillers have platelet-like structure, which improves the barrier properties of the polymer.[4] The platelets, because of the rise in temperature, are then evenly distributed into the polymer matrix, creating multiple parallel layers. The rise in temperature also affect the mobility of the polymeric chains and due to the motion of polymeric chains, the microvoids or vacant spaces present in the matrix are occupied by the readjustment of the nanoclay. These layers force the solvent molecules to flow through the polymer in a "torturous

path," forming complex barriers to the solvent molecules. The detailed process is shown in Scheme 1. The filler platelets are impenetrable for the diffusing solvent molecules. Therefore, when compared with the parent polymer, a decrease in the diffusion of solvent in the nanocomposites is observed.

Effect of linseed oil concentration

The plots for the mole percent uptake are shown in Figure 2 for the nanocomposite polymer samples at a temperature of 25 ± 1°C. In Figure 2, the oil contents vary from 30 to 70% in the samples and the content of surfactant (CTAB) modified montmorillonite is fixed at 5%. On increasing the oil contents in the polymers, the solvent uptake decreases in the matrix. Generally, with increasing oil contents in the polymer, crosslinking density decreases, leading to an increase in the solvent uptake.[27] In this case, the decrease in the solvent uptake with an increase in the oil contents can only be explained with a possible increase in the crosslink density, due to the presence of the fixed amount of nanofiller in the composition. The presence of nanoclay possibly increases the rate of reaction of linseed oil during the copolymerization, leading to an increase in the crosslink density. The increase in the crosslink density is confirmed latter during its calculation from the Flory-Rehner equation. Whereas, for the nanocomposites of tung oil-based polymers, a decrease in crosslink density (from 4.8×10^4 to 2.3×10^3 mol/m³, measured for DMA) is observed with an increase in tung oil content in the nanocomposite composition.[28] The possible reason for lower crosslink density from
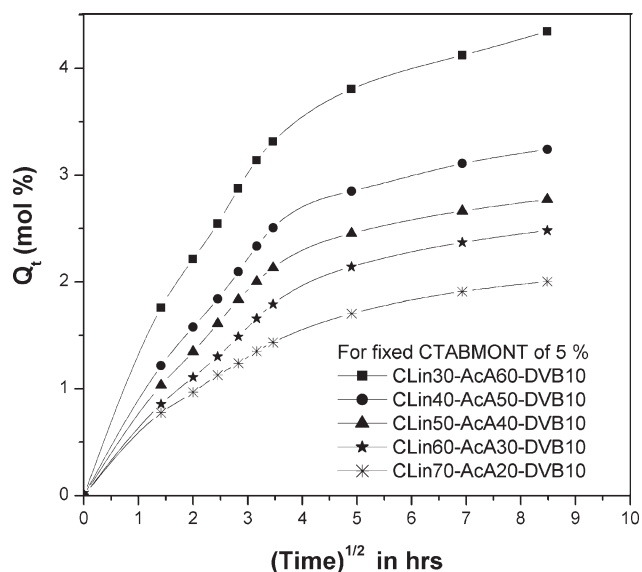
Figure 2 Sorption curve showing mole percent uptake of nanocomposite samples with 5% clay at 25°C.
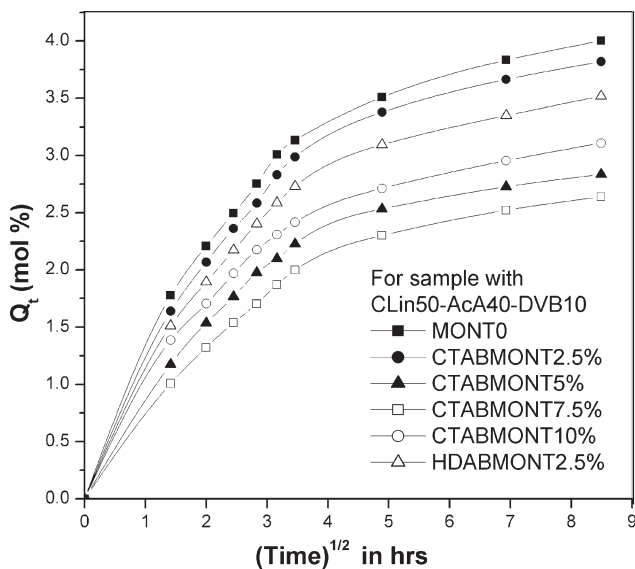
Figure 3 Sorption curve showing mole percent uptake of nanocomposite samples with variation in clay percentage from 0 to 10% at 25°C.

DMA is due to the prominence of plasticizing effect of increasing content of linseed oil.

The aforementioned findings have been confirmed during the thermal polymerization of conjugated linseed oil and a mixture of nanofiller with conjugated linseed oil. During the same period of heating (thermal polymerization), it has been observed that increase in viscosity is much higher in the case of nanoclay filled conjugated linseed oil compared to only conjugated linseed oil. This indicates that the rate of thermal polymerization increases a lot due to the presence of nanofiller. The nanofillers are nothing, but sodium and magnesium silicates $[M^+_y(Al_{2-y}$

Figure 5 Sorption curve showing mole percent uptake of nanocomposite samples with variation in clay percentage from 0 to 10% at 30°C.

$Mg_y)(Si_4)O_{10}(OH)_2*nH_2O]$. These cations, generally, help in the drying of linseed oil.[29–31]

In Figure 4, the solvent mole percent uptake is plotted against square root of time for different samples with a fixed clay (5 %) at 30°C. The samples with 30% and 70% oil contents show a maximum and a minimum solvent uptake, respectively. The same trend is also observed in Figures 6 and 8. The sample with 50% linseed oil shows intermediate swelling. All the samples show regular increase in swelling with time.

Effect of nanoclay

Figure 3 shows the mole percent uptake for the samples having the same polymer composition but with
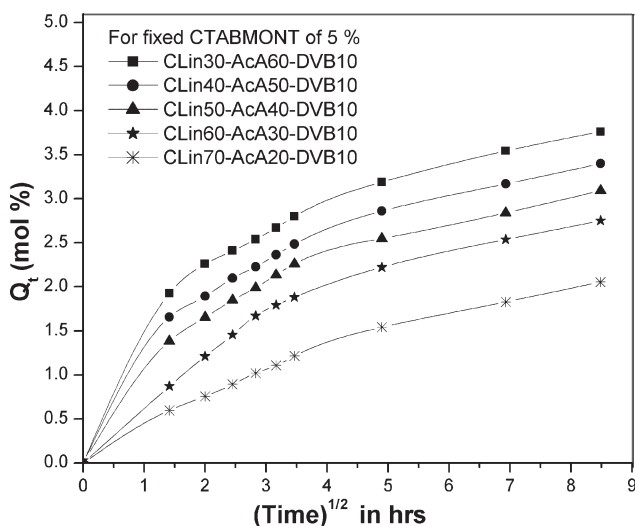
Figure 4 Sorption curve showing mole percent uptake of nanocomposite samples with 5% clay at 30°C.
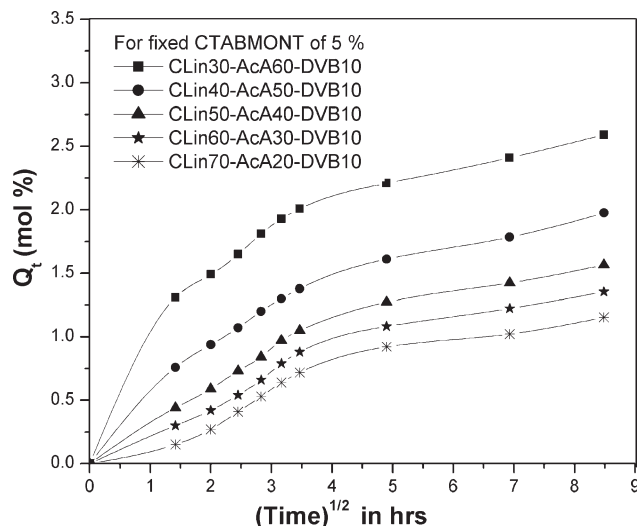
Figure 6 Sorption curve showing mole percent uptake of nanocomposite samples with 5% clay at 35°C.
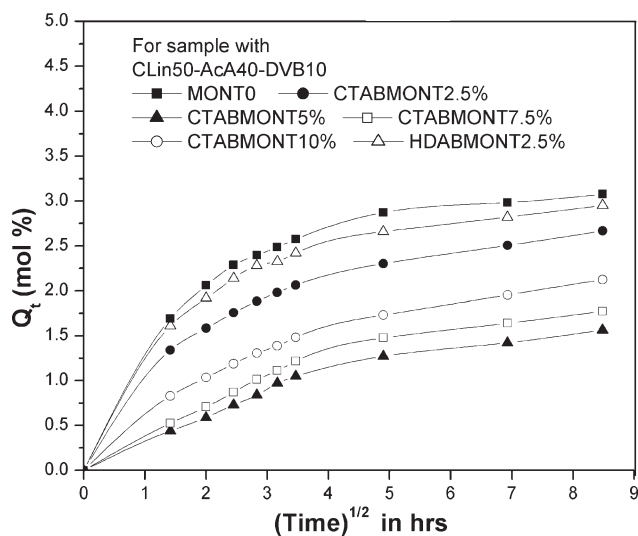
Figure 7 Sorption curve showing mole percent uptake of nanocomposite samples with variation in clay percentage from 0 to 10% at 35°C.

varying clay contents. In these samples, the sample without clay shows a maximum and the sample with 7.5% clay shows a minimum swelling. The sample with 10% nanoclay shows higher solvent uptake than the samples with 7.5% and 5% nanoclay contents. It is expected that a high loading of nanoclay is more effective for the solvent resistance, but the polymer with 10% filler shows high-solvent uptake. This may be due to the high nanoclay contents, resulting in the accumulation of clay at the interface. This behavior is similar to ordinary filler. The higher filler contents (10 %) reduce the barrier properties of the nanocomposite. Therefore, the sample shows distortion, instead of swelling after twelve
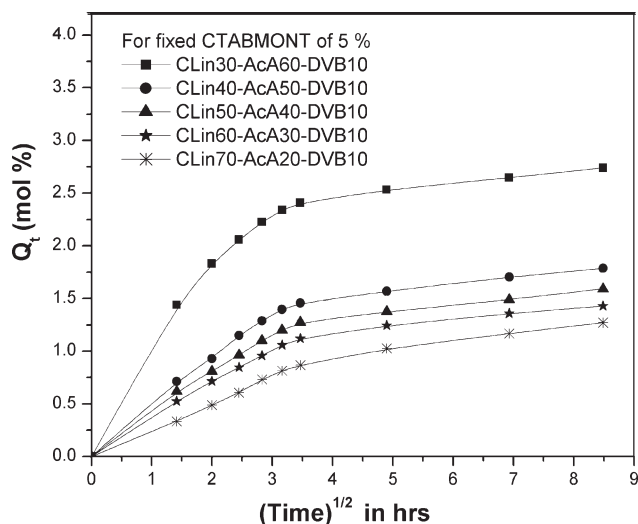
Figure 8 Sorption curve showing mole percent uptake of nanocomposite samples with 5% clay at 40°C.
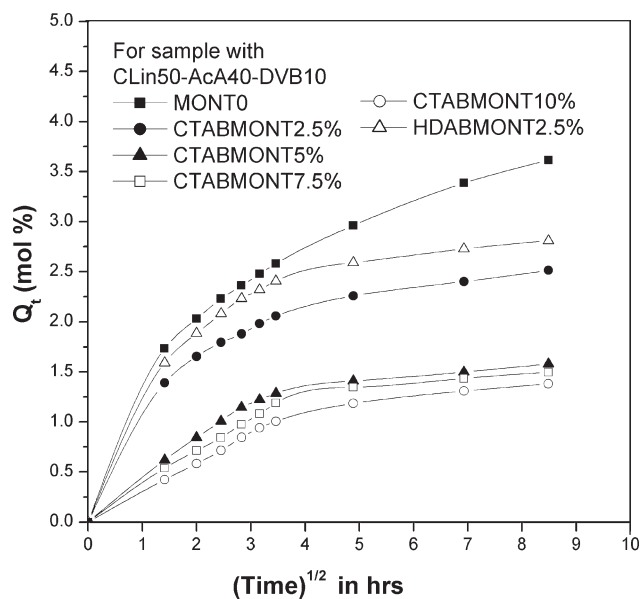
Figure 9 Sorption curve showing mole percent uptake of nanocomposite samples with variation in clay percentage from 0 to 10% at 40°C.

hours. The clay (montmorillonite) is modified by two surfactants, such as cetyl trimethyl ammonium bromide (CTAB) and hexadecyl ammonium bromide (HDAB). The samples with 2.5% of both modified clays show similar sorption curves, but the sample with CTABMONT shows more swelling than that with HDABMONT. It is apparent from Figure 3 that the clay-filled nanocomposites show less sorption than the sample without nanofiller. This indicates the enhancement in the barrier properties of the nanoclay filled polymer over the unfilled one. The
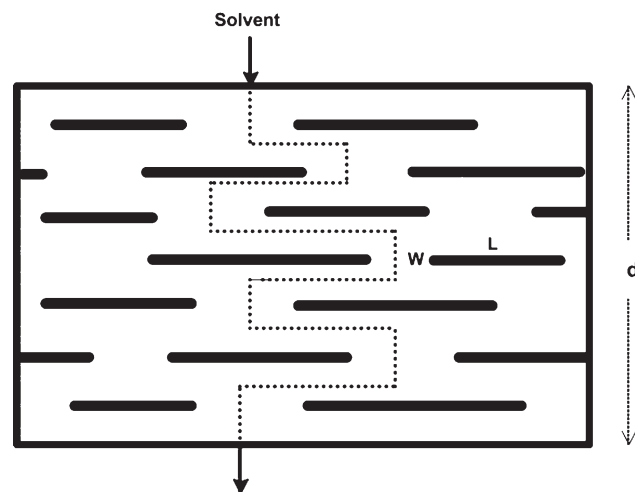
Scheme 1 The schematic representation of tortuosity-based model to describe the solvent diffusion in the nanoclay filled polymer composite. (W is the width or thickness and L is the length of the filler platelet. d is the thickness of the polymer matrix, through which the solvent molecules diffuse).
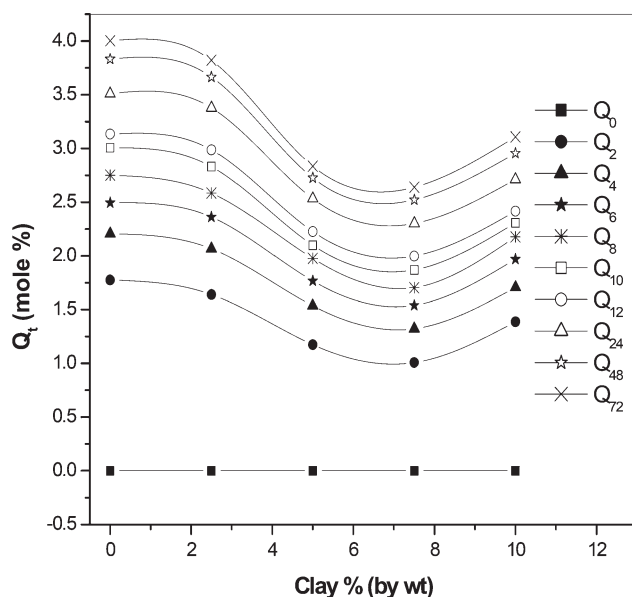
Figure 10 The plot of mole % uptake (Q_t) versus percentage of clay at 25°C.

increase in the barrier properties is due to the incorporation of nanoclay. The platelet-like structure with a high-aspect ratio can be expected to improve the resistance toward low molecular weight solvent molecules.

Figure 5 shows the variation of mole % uptake versus time at 30°C for varying ratio of nanoclay. The sample without nanoclay shows the highest swelling, and the sample with 7.5% nanoclay shows the lowest swelling during the whole period of experiment. In Figure 7, the maximum swelling is shown by the sample without nanoclay, followed by the sample with 2.5% nanoclay, and the minimum swelling is observed for the sample with 5% nanoclay. In Figure 9, the maximum swelling is shown by the sample without nanoclay, and the minimum swelling is shown by the sample with 10% nanoclay, closely followed by samples with 7.5 and 5% nanoclay.

Figure 10 shows the plot of mole % uptake (Q_t) versus percentage of clay at 25°C. It is observed in the figure that the samples show similar trends of mole percent uptake at all time intervals. For example, after 2 h, the maximum solvent uptake is for sample without nanoclay and then solvent uptake decreases gradually up to 7.5% clay contents. For 10% clay contents, the sample shows increase in the solvent uptake.

Diffusion kinetics

To find out the mechanism of swelling, the diffusion data is fitted into an empirical equation [eq. (3)][32] derived from equation of transport phenomena [eq. (2)][26]

$$\frac{Q_t}{Q_\infty} = kt^n \tag{2}$$

$$\ln \frac{Q_t}{Q_\infty} = \ln k + n \ln t \tag{3}$$

where Q_t and Q_∞ are the mole percent uptake of solvent at time "t" and at infinity or equilibrium. "k" is a constant, which depends upon both on the interaction between solvent and polymer and on the structure of polymer. In all cases, the regression coefficient (r) varies between 0.92 and 0.99. The values of constant "k" and "n" obtained from the eq. (3) and Q_∞ are represented in Table II. The value of "n" gives an idea of the mechanism of sorption.[33] When the value of n is 0.5, the mechanism of swelling is termed as Fickian transport. This occurs, when the rate of diffusion of solvent is less than that of polymer segmental mobility. The transport is considered as a non-Fickian, if the value of "n" is not "0.5." In particular, if "$n = 1$," the transport is called "Case II" transport.[33] It is a special case, where the solvent front moves with constant velocity. If "n" lies between "0.5" and "1," then it is called anomalous transport.[33] For non-Fickian transport, the diffusion is more rapid than the polymer relaxation rate. For anomalous transport, the diffusion and relaxation rates are comparable.[33] From Table II, the values of "n" fall below "0.5," indicating the transport as pseudo-Fickian.

The swelling data are used to calculate diffusion coefficient (D), which is a measure of the ability of solvent molecules to move into the polymer. The sorption coefficient (S), which gives an idea about the equilibrium sorption, is also calculated from the swelling data. The diffusion coefficient (D) is calculated as[34]

$$D = \pi \left(\frac{h\theta}{4Q_\infty} \right)^2 \tag{4}$$

where $\pi = 3.14$; h is the thickness of the dry sample, and θ is the slope of the initial linear portion of the curve Q_t versus $\sqrt{t}$; and Q_∞ is the mole percent uptake of the solvent at infinite time. The sorption coefficient (S) is calculated as[34]

$$S = \frac{M_\infty}{M_p} \tag{5}$$

where M_∞ is the mass of solvent uptake at equilibrium, and M_p is the mass of dry sample. The sorption and diffusion coefficients are used to calculate permeability coefficient (P) of samples, which is given by[34]

$$P = D \times S \tag{6}$$

Values of these coefficients are reported in Table III. The data in Table III indicates that the linseed oil

TABLE II
The Values of Mole Percent Uptake at Infinite Time (Q_∞), n, k and Standard
Deviation (SD) for Samples at Different Temperatures

Temperature (°C)	Sample ID	Q_∞ (mol %)	N	k	SD
25	CLin30	4.35	0.25	−0.98	0.08
	CLin40	3.24	0.27	−1.05	0.09
	CLin50	2.77	0.27	−1.05	0.09
	CLin60	2.48	0.30	−1.18	0.08
	CLin70	2.00	0.27	−1.07	0.06
	CTABMONT2.5	3.82	0.23	−0.91	0.07
	CTABMONT7.5	2.64	0.26	−1.03	0.08
	CTABMONT10	3.11	0.22	−0.87	0.06
	HDABMONT2.5	3.52	0.23	−0.91	0.07
	MONT0	4.00	0.22	−0.88	0.07
30	CLin30	3.76	0.19	−0.79	0.02
	CLin40	3.40	0.20	−0.85	0.02
	CLin50	3.09	0.22	−0.91	0.03
	CLin60	2.75	0.31	−1.22	0.09
	CLin70	2.05	0.35	−1.45	0.04
	CTABMONT2.5	3.59	0.16	−0.64	0.05
	CTABMONT7.5	2.39	0.25	−1.01	0.07
	CTABMONT10	2.70	0.23	−0.92	0.05
	HDABMONT2.5	3.33	0.21	−0.84	0.04
	MONT0	3.78	0.24	−0.96	0.03
35	CLin30	2.59	0.19	−0.78	0.04
	CLin40	1.98	0.26	−1.08	0.05
	CLin50	1.56	0.35	−1.40	0.10
	CLin60	1.35	0.42	−1.66	0.13
	CLin70	1.15	0.55	−2.08	0.23
	CTABMONT2.5	2.67	0.19	−0.76	0.04
	CTABMONT7.5	1.77	0.34	−1.33	0.10
	CTABMONT10	2.12	0.26	−1.06	0.04
	HDABMONT2.5	2.95	0.16	−0.64	0.05
	MONT0	3.08	0.18	−0.35	0.05
40	CLin30	2.74	0.16	−0.61	0.08
	CLin40	1.79	0.24	−0.92	0.11
	CLin50	1.59	0.25	−0.97	0.10
	CLin60	1.43	0.27	−1.03	0.11
	CLin70	1.27	0.36	−1.40	0.12
	CTABMONT2.5	2.51	0.16	−0.64	0.04
	CTABMONT7.5	1.50	0.28	−1.08	0.11
	CTABMONT10	1.38	0.33	−1.25	0.12
	HDABMONT2.5	2.81	0.15	−0.59	0.05
	MONT0	3.62	0.27	−0.79	0.05

contents influence the diffusion behavior of nanocomposites. It is observed that at a fixed nanoclay content (5 %), the sample with 50% oil shows a maximum and the sample with 30% linseed oil shows a minimum diffusion coefficient. For the variation in clay concentrations from 0 to 10%, the diffusion coefficient is observed to be maximum and minimum for the sample with 0% clay (virgin polymer), 7.5% clay, respectively. The diffusion coefficient is inversely proportional to the mole percent uptake of the solvent [eq. (4)]. The experimental results indicate that the diffusion of the solvent through nanocomposite decreases with increasing clay contents up to 7.5%. When the clay contents are 10%, the sample shows an increase in the diffusion. This is due to the

high filler contents, which increases the uneven distribution of the filler in the matrix. This results in the accumulation of the filler at the interface, causing in a net decrease in the barrier properties.[35] But, the diffusion coefficient for sample (with 10% nanoclay) is higher than that for neat polymer. The diffusion coefficient shows an increase with an increase in the temperature. In case of sample CLin30, the diffusion coefficient is the lowest at 25°C, which keeps on increasing with temperature and increases almost two fold at 40°C. For the modification of montmorillonite clay, two types of surfactants are used, CTAB and HDAB. When samples with these two modified nanofillers are compared, both show a similar diffusion behavior. At all temperatures, the

TABLE III
Diffusion Coefficient (*D*), Sorption Coefficient (*S*) and Permeability Coefficient (*P*) in THF for the Samples at Different Temperatures

Temperature (°C)	Sample ID	$D \times 10^5$ (cm^2/s)	S (g/g)	$P \times 10^5$ (cm^2/s)
25	CLin30	2.81	1.62	4.55
	CLin40	3.40	1.75	5.95
	CLin50	3.67	1.80	6.61
	CLin60	3.35	2.25	7.54
	CLin70	3.46	1.93	6.68
	CTABMONT2.5	3.14	1.84	5.78
	CTABMONT7.5	3.57	2.39	8.53
	CTABMONT10	3.49	2.02	7.05
	HDABMONT2.5	3.26	1.02	3.33
	MONT0	1.89	1.45	2.74
30	CLin30	2.81	1.83	5.14
	CLin40	2.89	2.11	6.10
	CLin50	3.06	1.16	3.55
	CLin60	3.14	2.30	7.22
	CLin70	2.42	1.13	2.73
	CTABMONT2.5	3.47	1.58	5.48
	CTABMONT7.5	3.54	1.76	6.23
	CTABMONT10	3.42	1.92	6.57
	HDABMONT2.5	3.17	1.71	5.42
	MONT0	1.87	1.74	3.25
35	CLin30	3.59	1.81	6.50
	CLin40	3.27	1.22	3.99
	CLin50	3.28	0.96	3.15
	CLin60	3.13	0.75	2.35
	CLin70	3.13	0.93	2.91
	CTABMONT2.5	3.56	1.72	6.12
	CTABMONT7.5	3.37	1.09	3.67
	CTABMONT10	3.25	1.18	3.84
	HDABMONT2.5	3.80	2.08	7.90
	MONT0	1.85	2.15	3.98
40	CLin30	4.51	1.97	8.88
	CLin40	4.71	1.18	5.56
	CLin50	4.57	1.45	6.63
	CLin60	4.48	1.10	4.93
	CLin70	3.64	0.90	3.27
	CTABMONT2.5	3.96	1.71	6.77
	CTABMONT7.5	4.37	1.03	4.50
	CTABMONT10	3.98	1.01	4.02
	HDABMONT2.5	4.13	2.11	8.71
	MONT0	1.74	2.83	4.92

sample without nanoclay (virgin polymer) shows twofold decrease in the diffusion coefficient than nanoclay filled sample (7.5 %).

In case of sorption by the samples, any particular trend is observed, and it is quite difficult to explain this behavior. At 25 and 30°C, the sorption coefficient increases with an increase in the linseed oil contents. The samples with 30 and 60% oil contents show a minimum and maximum sorption coefficient, respectively. When the clay contents are varied from 0 to 10%, the samples without clay[27] and with 7.5% clay content show a minimum and a maximum sorption coefficient, respectively.

At 35 and 40°C, the samples show a decrease in the sorption coefficients with an increase in the oil contents. A small increase in the sorption coefficient with an increase in the temperature is observed. The sorption coefficient is maximum and minimum for the sample with 30% and 60% oil composition, respectively. This indicates the increase in sorption with an increasing oil contents. At these temperatures, the sorption in the nanocomposites shows an increase with increasing clay contents. The sorption coefficient is observed to be maximum and minimum for the sample without clay and 7.5% clay, respectively. Other samples show intermediate sorption coefficients. The sorption coefficient is a direct indicator of the absorbed solvent in the polymer. The increase in the sorption coefficient with temperature indicates the increase in the solvent absorption capacity of the nanocomposite material.

In all of the systems, it is observed that the sorption and diffusion coefficients decrease with an increase in the temperature. It is reported

elsewhere[36] for natural rubber that these coefficients show an increase with a raise in the temperature. But in our case, these coefficients decrease with temperature. This can be explained by the dual mode model for diffusion in the polymers below glass transitions.[37] According to this model, glassy polymers contain a distribution of microvoids frozen into a structure as the polymer is cooled through its glass transition temperature. The free segmental rotations of the polymer chains in the glassy state are restricted, which results in the fixed microvoids throughout the polymer. The microvoids in the glassy polymer network immobilize the solvent molecules by entrapment. These entrapments increase the size of the polymer, resulting in the enlargement of the microvoids. The enlargement of microvoids further leads to initiate the macrofractures in the polymer.

The permeability coefficients of the samples are the product of diffusion and sorption coefficients. The permeability coefficients in samples show an increase with the increasing amount of linseed oil. The permeability coefficient also increases with an increase in temperature. At 25°C, the permeability coefficient is observed to be minimum and maximum for the sample CLin30 and CLin60, respectively. At this temperature, the permeability coefficient shows an increase with an increase in the clay contents. The sample without clay shows a minimum and the sample with 7.5% clay shows a maximum permeability coefficient. At 30°C, the permeability coefficient is observed to be maximum and minimum for CLin60 and CLin70 sample, respectively. When clay concentration is varied for a fixed composition polymer, the permeability coefficient is observed to be minimum and maximum for the sample without clay and with 10% clay, respectively. At 35°C, the samples show a decrease in permeability coefficient with an increase in the oil contents. The permeability coefficient is observed to be maximum and minimum for sample with 30% and 70% oil, respectively. It is observed that the permeability coefficient is maximum and minimum for sample with 2.5% and 5% clay. At 40°C, the permeability coefficient also decreases with an increase in the oil contents. The permeability coefficient is maximum and minimum for the sample with 30% and sample 70% oil, respectively. At this temperature, the permeability coefficient shows a decrease with an increase in clay content and it is observed to be maximum and minimum for the sample with 2.5% and 10% clay content, respectively.

Crosslink density and molecular weight

The sorption data are also used to calculate the crosslink density of the polymer networks using

TABLE IV
Volume Fraction of Polymer (V_p), Crosslink Density (v) and Molecular Weight Between Two Crosslinks ($\overline{M}_c$) for the Different Polymeric Nanocomposites at 25°C

Sample ID	V_p	$v \times 10^6$ (mol/cm^3)	$\overline{M}_c \times 10^{-9}$ (cm^3/ mol)
CLin30	0.33	101.07	4.95
CLin40	0.36	124.03	4.03
CLin50	0.26	170.56	2.93
CLin60	0.26	181.46	2.76
CLin70	0.23	183.39	2.73
CTABMONT2.5	0.31	161.80	3.09
CTABMONT7.5	0.27	237.46	2.11
CTABMONT10	0.28	169.56	2.95
HDABMONT2.5	0.91	151.77	3.29
MONT0	0.22	25.93	19.28

Flory-Rehner's equation[38]

$$v = -\frac{\ln(1 - V_p) + V_p + \chi V_p^2}{V_1(V_p^{1/3} - 0.5V_p)} \quad (7)$$

where V_p is the volume fraction of the polymer in the mixture, χ is the polymer-solvent interaction parameter, and V_1 is the molar volume of the solvent. V_p and χ are obtained by the following equations[38]

$$V_p = \frac{\text{(Weight of polymer/Density of polymer)}}{\begin{array}{c}\text{(Weight of polymer/Density of polymer}\\+ \text{Weight of solvent/Density of solvent)}\end{array}} \quad (8)$$

$$\chi = \chi_H + \chi_S = \frac{V_1(\delta_p - \delta_s)^2}{RT} + 0.34 \quad (9)$$

where χ_H and χ_S are the enthalpic and entropic components of χ, δ_1 and δ_2 are the solubility parameters of polymer and solvent, respectively. The solubility parameter of the polymer is obtained by fitting the swelling coefficients of the polymer in various solvents. The results are reported in Table IV. The molecular weight between two crosslinks ($\overline{M}_c$) is also calculated for all the samples by the following equation[36]

$$\overline{M}_c = \frac{1}{2v} \quad (10)$$

The values of the crosslink density and $\overline{M}_c$ are reported in Table IV. The crosslink density and the molecular weight between two crosslinks are in good agreement with the sorption kinetics. The crosslink density increases and molecular weight between two crosslinks decreases with an increase in the oil contents (at 5% clay concentration). The crosslink density is observed to be minimum and maximum for the sample with 30% (CLin30) and 70% linseed oil (CLin70), respectively. The molecular
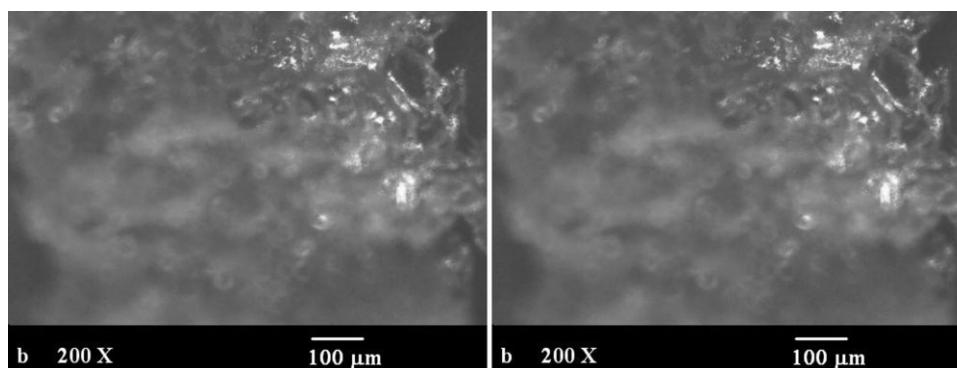
Figure 11 Micrographs of the swelling of the nanocomposite sample containing conjugated linseed oil 50%, acrylic acid 40%, and divinylbenzene 10% and 5% clay (sample CLin50).

weight between two crosslinks is maximum for sample without clay and minimum for sample with 7.5% clay. The variation in clay concentration affects the crosslink density. It is observed that the crosslink density increases more than sixfold on addition of 2.5% nanoclay. The crosslink density is observed to be a minimum and a maximum for the sample without nanoclay (MONT0) and with 7.5% nanoclay (CTABMONT7.5), respectively, whereas, the molecular weight between two crosslinks is minimum for sample with 7.5% clay (CTABMONT7.5) and maximum for sample without clay (MONT0). The sample with 10% nanoclay (CTABMONT10) shows slightly less crosslink density and molecular weight between two crosslinks than the sample with 7.5% nanoclay (CTABMONT7.5). The increase in the crosslink density and the increase in barrier properties explains the cause of increase in the sorption resistance with an increase in the oil content.

Optical micrographs of the samples

Figure 11 shows the micrographs of the polymer nanocomposite samples at 60 and 200X magnification (scale 100 µm) immediately after the completion of the sorption experiments. In Figure 11(a), smooth surface is observed for CLin50 sample and at a higher magnification of 200X [Fig. 11(b)], shining gel-like appearance can clearly be observed. This is the clear evidence that the nanocomposite have resisted the solvent and therefore swelling is less than the sample without clay.

CONCLUSION

The solvent-resistance properties of the montmorillonite-filled conjugated linseed oil-based nanocomposites are studied in tetrahydrofuran through equilibrium swelling method at different temperatures. The values of "n" in the transport equation are found to be below "0.5," showing the non-Fickian diffusion in the polymer. The dependence of the diffusion coefficient on the composition, percentage of clay, and temperature has been studied for the nanocomposite samples. The crosslink density of the nanocomposites ranges from 101.07 to 237.46 $\times$ 10^6 mol/cm^3.

References

1. Lange, J.; Wyser, Y. Packaging Technol Sci 2003, 16, 149.
2. Ray, S.; Okamoto, K.; Okamoto, M. Macromolecules 2003, 36, 2355.
3. Giannelis, E. P. Adv Mater 1996, 8, 29.
4. Lu, C.; Mai, Y. W. Phys Rev Lett 2005, 95, 088303.
5. Saminathan, K.; Selvakumar, P.; Bhatnagar, N. Polym Test 2008, 27, 296.
6. Wilkinson, A. N.; Man, Z.; Stanford, J. L.; Matikainen, P.; Clemens, M. N.; Lees, G. C.; Liauw, C. M. Compos Sci Technol 2007, 67, 3360.
7. Drown, E. K.; Mohanty, A. K.; Parulekar, Y.; Hasija, H.; Harte, B. R.; Misra, M.; Kurian, J. V. Compos Sci Technol 2007, 67, 3168.
8. Bergaya, F. A. Micropor Mesopor Mater 2008, 107, 141.
9. Xue, S.; Pinnavaia, T. J. Micropor Mesopor Mater 2008, 107, 134.
10. Ding, Y.; Zhang, X.; Xiong, R.; Wu, S.; Zha, M.; Tang, H. Eur Polym J 2008, 44, 24.
11. Syzdek, J.; Borkowska, R.; Perzyna, K.; Tarascon, J. M.; Wieczorek, W. J Power Sources 2007, 173, 712.
12. Ahmadi, B.; Kassiriha, M.; Khodabakhshi, K.; Mafi, E. R. Prog Org Coat 2007, 60, 99.
13. Eitan, A.; Fisher, F. T.; Andrews, R.; Brinson, L. C.; Schadler, L. S. Compos Sci Technol 2006, 66, 1162.
14. Hackman, I.; Hollaway, L. Proceedings of the International Symposium on Bond Behaviour of FRP in Structures (BBFS); International Institute for FRP in Construction; 2005, 525.
15. Zhu, Q.; Shentu, B.; Liu, Q.; Weng, Z. Eur Polym J 2006, 42, 1417.
16. Detallante, V.; Langevin, D.; Chappey, C.; Metayer, M.; Mercier, R.; Pineri, M. Desalination 2002, 148, 333.
17. Kumar, R.; Srivastava, S. K.; Mathur, G. N. J Elastomers Plast 1985, 17, 89.
18. Han, H.; Gryte, C. C.; Ree, M. Polymer 1995, 36, 1663.
19. Singh, P.; Kaushik, A.; Gupta, P. J Reinforced Plast Compos 2005, 24, 1479.
20. Sen, M.; Guven, O. Comput Theor Polym Sci 2000, 11, 475.
21. Singh, P. P.; Cushman, J. H.; Maier, D. E. Chem Eng Sci 2003, 58, 2409.
22. Altinkaya, S. A.; Ramesh, N.; Duda, J. L. Polymer 2006, 47, 8228.

23. Fieldson, G. T.; Barbari, T. A. Polymer 1993, 34, 1146.
24. Philippe, L.; Sammon, C.; Lyon, S. B.; Yarwood, J. Prog Org Coat 2004, 49, 302.
25. Philippe, L.; Sammon, C.; Lyon, S. B.; Yarwood, J. Prog Org Coat 2004, 49, 315.
26. Ajithkumar, S.; Patel, N. K.; Kansara, S. S. Polym Gels Networks 1998, 6, 137.
27. Sharma, V.; Banait, J. S.; Kundu, P. P. J Appl Polym Sci 2008, 111, 1816.
28. Kundu, P. P.; Larock, R. C. Industrial & Engineering Chemistry Research 2008, 47, 8566.
29. Evans, W. L.; Marling, P. E.; Lower, S. E. Ind Eng Chem Res 1927, 19, 640.
30. Clark, G. L.; Tschentke, H. L. Ind Eng Chem Res 1929, 21, 621.
31. Currier, A. J.; Kagarise, I. H. Ind Eng Chem Res 1937, 29, 467.
32. George, S. C.; Knorgen, M.; Thomas, S. J Membr Sci 1999, 163, 1.
33. Crank, J.The Mathematics of Diffusion, 2nd ed.; Clarendon Press: Oxford, 1975.
34. Ajithkumar, S.; Patel, N. K.; Kansara, S. S. Eur Polym J 2000, 36, 2387.
35. Sharma, V.; Banait, J. S.; Kundu, P. P. Polym Compos, to appear.
36. Mathew, A. P.; Packirisamy, S.; Kumaran, M. G.; Thomas, S. Polymer 1995, 36, 4935.
37. Meares, P. J Am Chem Soc 1954, 76, 3415.
38. Zhu, L.; Wool, R. P. Polymer 2006, 47, 8106.